

## Heat Transfer Enhancement of an Automobile Engine Radiator using ZnO Water Base Nanofluids

Muhammad QASIM<sup>1</sup>, Muhammad SAJID KAMRAN<sup>1</sup>, Muhammad AMMAR<sup>2\*</sup>, Muhammad ALI JAMAL<sup>2</sup>, Muhammad YASAR JAVAID<sup>3</sup>

1. Department of Mechanical Engineering, University of Engineering and Technology, Lahore 54890, Pakistan

2. Department of Chemical Engineering Technology, Government College University, Faisalabad 38000, Pakistan

3. Department of Mechanical Engineering Technology, Government College University, Faisalabad 38000, Pakistan

© Science Press, Institute of Engineering Thermophysics, CAS and Springer-Verlag GmbH Germany, part of Springer Nature 2020

**Abstract:** In this research paper, the forced convective heat transfer enhancement of a Suzuki Mehran (VXR) 2016 radiator (heat exchanger) along with pressure drop and friction factor by utilizing Zinc oxide (ZnO) water based nanofluids has been experimentally studied. Three types of nanofluids with different volumetric concentrations of ZnO nanoparticles (0–0.3%) were employed in order to understand its effect on heat transfer enhancement. The experimental setup was completely designed as closely as possible to the car cooling system. The experimentation has been done under laminar flow conditions ( $186 \leq Re \leq 1127$ ) at different fluid volume flow rates (2–12 L/min) and constant fluid inlet temperature (70°C) to the automobile radiator. A maximum enhancement in heat transfer rate, overall heat transfer coefficient and Nusselt number was obtained up to 41%, 50% and 31% by using nanofluid with 0.2% volumetric concentration of nanoparticles respectively. On the other hand, the mean enhancement in pressure drop and friction factor was obtained up to 47% and 46% by using nanofluid with the same volumetric concentration of nanoparticles i.e. 0.2% respectively. The experimental results also revealed that the heat transfer rate, overall heat transfer coefficient and Nusselt number of nanofluids increases by increasing the volume flow rates and volumetric concentration of nanoparticles. However, these thermal performance parameters of nanofluids started to decline when the volumetric concentration of nanoparticles was increased from 0.2% to 0.3%. Furthermore, pressure drop and friction factor of nanofluids increase by increasing the volumetric concentration of nanoparticles, while pressure drop increases and friction factor decreases by increasing the volume flow rate of nanofluids respectively. At the end, the thermal efficiency of automobile radiator with high cooling rates was obtained by using nanofluid with 0.2% volumetric concentration of nanoparticles.

**Keywords:** ZnO, nanoparticles, heat transfer enhancement, thermal efficiency, automobile radiator

### 1. Introduction

Scientists and engineers have been taking massive interest to augment the heat transfer in various industrial

devices in order to enhance their thermal efficiency for a long time. In the past, various methods like extended surfaces and natural and forced convection were employed for heat transfer at a superior rate. In the

<b>Nomenclature</b>			
$A$	Area of radiator tube/m <sup>2</sup>	$\dot{V}$	Volumetric flow rate/m <sup>3</sup> ·s <sup>-1</sup>
$C_p$	Specific heat/kJ·kg <sup>-1</sup> ·K <sup>-1</sup>	$v$	Flow velocity/m·s <sup>-1</sup>
$D$	Major diameter of radiator tube/m	$W$	Width/in.
$d$	Minor diameter of radiator tube/m	$W_p$	Pumping power/mW
$d_H$	Hydraulic diameter of radiator tube/m	<b>Greek Symbols</b>	
$f$	Friction factor	$\mu$	Viscosity/N·s·m <sup>-2</sup>
$g$	Gravitational acceleration/m·s <sup>-2</sup>	$\rho$	Density/kg·m <sup>-3</sup>
$H$	Height/in.	$\phi$	Volumetric concentration of nanoparticles/%
Hg	Mercury	<b>Subscripts</b>	
$h$	Heat transfer coefficient/W·m <sup>-2</sup> ·K <sup>-1</sup>	b	Bulk
$\Delta h$	Manometer reading/mm	c	Cross
$k$	Thermal conductivity/kW·m <sup>-1</sup> ·K <sup>-1</sup>	Hg	Mercury
$L$	Length of radiator tube/m	in	Inlet
$LMTD$	Logarithmic mean temperature Difference/K	nf	Nanofluid
$\dot{m}$	Mass flow rate/kg·s <sup>-1</sup>	out	Outlet
$Nu$	Nusselt number	p	Nanoparticle
$n$	Number of radiator tubes	s	Surface
$P$	Perimeter of radiator tube/m	wa	Wall
$\Delta P$	Pressure drop/Pa	w	Water
$Pr$	Prandtl number	<b>Acronyms</b>	
$Q$	Heat transfer rate/W	AC	Alternate Current
$Re$	Reynolds number	CNT	Carbon Nanotube
$T$	Temperature/K	DC	Direct Current
$\Delta T$	Temperature difference/K	MWCNTs	Multi-Walled Carbon Nanotubes
$U$	Overall heat transfer coefficient/W·m <sup>-2</sup> ·K <sup>-1</sup>	TEM	Transmission Electron Microscope
$u$	Volume flow rate/L·min <sup>-1</sup>		

present era, scientists and engineers introduced a new term for enhancement of heat transfer, which is termed as nano-fluids. They contain nanoparticles having a size range of 10–100 nanometer (nm) scattered in their base liquids [1]. Nanofluids have showed excellent thermal properties and displayed superior heat transfer characteristics as compared to the conventional heat transfer fluids [2].

Radiators are one of the general examples of heat exchangers, which have numberless applications ranging from automobiles to various industrial machines. Radiator is a major part of an automobile, whose purpose is to provide cooling of engine. Its configuration consists of flat tube and louvered fin and because of its complex structure, a few experimental studies are available [2]. Traditional use of coolants, e.g. water or ethylene glycol in radiator has less potential of effective heat transfer. Therefore, resultantly, unremoved heat increases the temperature of the engine, which results into high fuel

consumption and thermal deterioration of engine parts. Hence, the life of the engine reduces rapidly [3]. In order to overcome these fuel and mechanical losses and to improve the thermal efficiency of engine, many scientists and engineers used nanofluids in the automobile radiator as a new working coolant instead of traditional ones [4,5].

Leong et al. [6] experimentally studied the implementation of Copper (Cu) ethylene glycol nanofluids in a car radiator and reported that the heat transfer rate and overall heat transfer coefficient were enhanced up to 3.8%. They also reported that the pumping power was enhanced up to 12.13% after the utilization of Cu ethylene glycol nanofluids. Peyghambarzadeh et al. [7] improved the automobile radiator cooling performance by using Aluminium oxide (Al<sub>2</sub>O<sub>3</sub>) water nanofluids and reported a 45% enhancement in its thermal efficiency. Peyghambarzadeh et al. [8] experimentally studied the heat transfer by utilizing Copper oxide (CuO) and Iron oxide (Fe<sub>2</sub>O<sub>3</sub>) water nanofluids through a car radiator.

They reported a 9% increase in overall heat transfer coefficient by using of  $\text{Fe}_2\text{O}_3$  water nanofluids. Naraki et al. [9] experimentally studied the application of Copper oxide (CuO) water nanofluids in a car radiator and concluded that the overall heat transfer coefficient for car radiator was enhanced up to 8% after the utilization of CuO water nanofluids.

Hussein et al. [10] experimentally studied the heat transfer in Silicon dioxide ( $\text{SiO}_2$ ) water nanofluids through a car radiator and observed that the heat transfer rate, Nusselt number and friction factor were increased up to 50%, 40% and 15% by the utilizations of  $\text{SiO}_2$  water nanofluids. Nieh et al. [11] experimentally investigated the heat dissipation performance of air cooled radiator by using Aluminium oxide ( $\text{Al}_2\text{O}_3$ ) and Titanium dioxide ( $\text{TiO}_2$ ) nano-coolants. They proved that the overall heat dissipation performance of the system was enhanced by the utilization of  $\text{Al}_2\text{O}_3$  and  $\text{TiO}_2$  nano-coolants. Teng and Yu [12] experimentally investigated the heat dissipation performance of multi-walled carbon nanotubes (MWCNTs) nano-coolants through a motorcycle radiator. They reported that the heat dissipation performance, efficiency factor and pumping power were increased up to 12.8%, 14.1% and 4.9% by using of MWCNTs nano-coolants. Chavan and Pise [13] experimentally studied the implementation of Aluminium oxide ( $\text{Al}_2\text{O}_3$ ) water nanofluids in a car radiator. They reported that the heat transfer efficiency of radiator was enhanced up to 40%–45% by the utilization of  $\text{Al}_2\text{O}_3$  water nanofluids. Heris et al. [14] experimentally studied the heat transfer in Copper oxide (CuO) nanofluids through a car radiator. They all concluded that the thermal efficiency of radiator was increased up to 55% by the utilization of CuO nanofluids. Ebrahimi et al. [15] experimentally studied the heat transfer in Silicon dioxide ( $\text{SiO}_2$ ) water nanofluids and reported that the Nusselt number was enhanced up to 9.3% by using of  $\text{SiO}_2$  water nanofluids. Chougule and Sahu [16] experimentally studied the automobile radiator cooling performance by using Aluminium oxide ( $\text{Al}_2\text{O}_3$ ) and Carbon nanotube (CNT) water nanofluids. They reported that the thermal conductivity and Nusselt number were increased up to 60% and 90.76% by using of CNT water nanofluids. They also reported that the thermal conductivity and Nusselt number were increased up to 12% and 52.03% by using of  $\text{Al}_2\text{O}_3$  water nanofluids.

The literature study proves that the use of nanoparticles or nanofluids in an automobile radiator is well established and thoroughly studied and reported. Suzuki Mehran (VXR) is a locally manufactured automobile in Pakistan. The car's engine is 800cc. Pakistan is located in a dry and hot climate region. Due to excessive heat in summer, there is a strong need of good and efficient coolant in radiator to remove

excessive heat from engine and extend engine life. Moreover, a good heat transfer increases the fuel efficiency of an engine. In this research work, the thermal performance parameters like heat transfer rate, overall heat transfer coefficient and Nusselt number along with pressure drop and friction factor of ZnO water base nanofluids were experimentally studied. The experimental setup was fully designed as closer as possible to the vehicle cooling system. Furthermore, three types of nanofluids with various volumetric concentrations of ZnO nanoparticles (0–0.3%) were utilized and all the experiments were performed under laminar flow conditions ( $186 \leq Re \leq 1127$ ) at various fluid volume flow rates (2–12 L/min) and constant radiator fluid inlet temperature ( $70^\circ\text{C}$ ) in order to thoroughly understand the heat transfer performance as well as pressure drop and friction factor of these nanofluids in the automobile radiator.

## 2. Experimental

### 2.1 Preparation of nanofluids

In this experimental work, four types of fluids were used. The 1<sup>st</sup> one is pure water and remaining three are ZnO nanofluids having water as base fluid. The ZnO nanoparticles were purchased from chemical market and prepared water base ZnO nanofluids with different volumetric concentrations of nanoparticles (0.1%, 0.2% and 0.3%) from chemical laboratory of Pakistan Council of Scientific and Industrial Research (PCSIR), Laboratories Complex, Lahore, Pakistan. These nanofluids were prepared via two step method. In this method, ZnO nanoparticles were initially dissolved into pure water by keeping the pH value of water at approximately 2. Afterward a constant stirring was done for 2–3 hours with the help of magnetic stirrer. For the prevention of nanoparticles agglomeration, a process of sonication was further carried out for 2–3 hours with the help of ultrasonic cleaner. This process provided a homogenous and stable water base ZnO nanofluid. These nanofluids were well stable even after 4–5 days. The ZnO nanoparticles thermo-physical properties are given in Table 1. Few of these thermo-physical properties of nanoparticles were utilized to determine the desired input parameters of nanofluids. Transmission electron microscope (TEM) micrograph of ZnO nanoparticles was obtained using JEM-2100F transmission electron microscope at 200 kV. From Fig. 1, it can be clearly seen that the morphology of ZnO nanoparticles is almost spherical.

### 2.2 Experimental setup

The schematic flow diagram of experimental setup is illustrated in Fig. 2. The experimental setup consists of

**Table 1** Thermo-physical properties of ZnO nanoparticles [17]

Parameter	Value
Purity/%	99.5
Particle approximate size/nm	20
Specific surface area/m <sup>2</sup> ·g <sup>-1</sup>	50
Bulk density/g·cm <sup>-3</sup>	0.3–0.45
True density/g·cm <sup>-3</sup>	5.606
Thermal conductivity/W·m <sup>-1</sup> ·K <sup>-1</sup>	110.95
Specific heat/J·kg <sup>-1</sup> ·K <sup>-1</sup>	502.7
Melting point/°C	1975
Boiling point/°C	2360
Color	Milky white
Morphology	Nearly spherical
Odor	Odorless

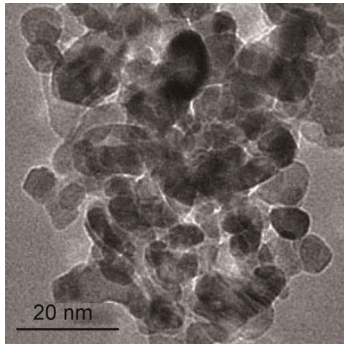


**Fig. 1** TEM micrograph of ZnO nanoparticles

a Suzuki Mehran (VXR) 2016 radiator (heat exchanger), a centrifugal pump (single-stage), a storage tank, an electric water heater with stem thermostat (single-pole), a ball valve (drain valve), two gate valves, an electric cooling fan (DC), a power supply (AC), a rota meter used as flow meter, a manometer (U-tube), twelve type K thermocouples with digital display temperature controller (REX-C100), a control panel and fluid transport pipes.

In this experimental work, radiator of Suzuki Mehran (VXR) 2016 is used. It consists of 33 vertical flattened Aluminium (Al) tubes with a large number of Aluminium fins on the outer surface of these tubes. The cooling of radiator is done by using a DC electric fan with an operating speed of (800–900 r/min). The electric fan utilized in this experimental setup is the same as utilized in common automobile radiators. The dimensions of automobile radiator are given in Table 2.

A single-stage centrifugal pump (VALCO-55CG) with maximum rated head of 21.5 m and maximum flow rate of 20 L/min is used. Its inlet flow line is connected to the storage tank and outlet flow line is connected to the bypass line and automobile radiator. The main purpose of this centrifugal pump is to circulate the working fluid in a close loop via fluid transport pipes. The fluid transport pipes with different diameters are employed to provide the flow passage of working fluid. A storage tank, which is constructed from mild steel having dimensions are 8 in. × 24 in. × 13 in. (*L* × *W* × *H*), is used to reserve and provide fluid to the centrifugal pump. In order to minimize the heat losses, insulation is made on the storage tank. An electric water heater (R-T-M) with power input of 1500 W is used. It is placed inside the storage tank in such a

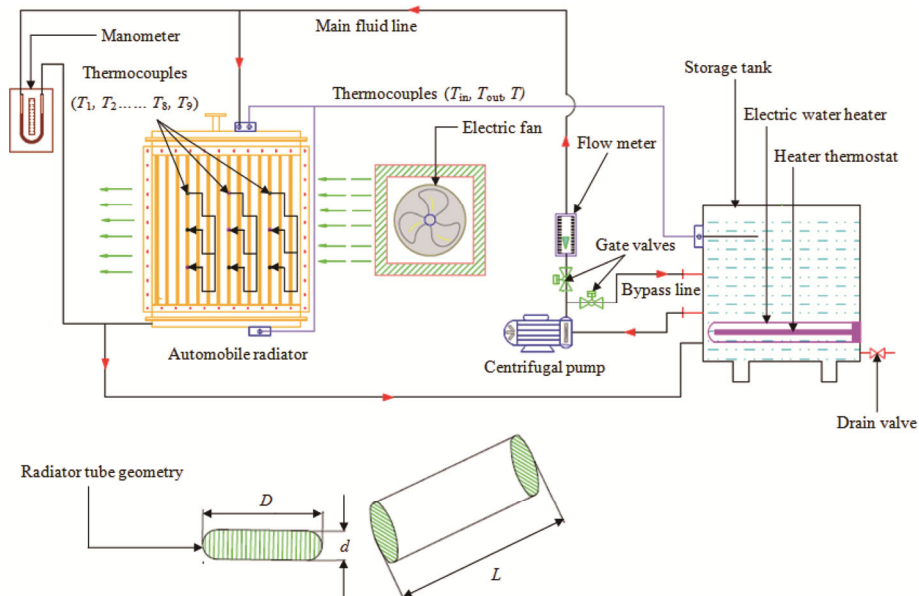


**Fig. 2** Schematic flow diagram of experimental setup

**Table 2** Dimensions of automobile radiator

Parameter	Value
Length×Width ×Height/mm	370×39×390
Major diameter of tube/mm	25.4
Minor diameter of tube/mm	2.0
Length of tube/mm	313
Cross sectional area of tube/mm <sup>2</sup>	49.9416
Hydraulic diameter of tube/mm	3.7632
Perimeter of tube/mm	53.0831
Surface area of tube/mm <sup>2</sup>	16 614.9790

way that its heating element is fully-dipped into the working fluid. The main purpose of this electric heater is to heat the working fluid of storage tank at desired temperature with the help of a single-pole stem heater thermostat having a temperature limit of 20°C to 80°C and accuracy of ±1°C.

A ball valve, which is mounted on the bottom side of storage tank, is used to drain the fluid of storage tank. Two gate valves are also used. The 1<sup>st</sup> one is placed on the main fluid line, which is connected to the automobile radiator and the 2<sup>nd</sup> one is placed on the bypass line also known as bypass valve, which is connected to the storage tank. The major purpose of these gate valves is to adjust the fluid flow rate at desired level with the help of a bypass line, which is installed to pass the additional fluid back to the storage tank. A rotameter (LZT-1005M) with measurement capacity in the range of 2–18 L/min having an accuracy of ±4% is used. Only desired flow rate of working fluid is then passed through the automobile radiator via rota meter with the help of centrifugal pump. It is placed on the main fluid line, which is connected to the automobile radiator. The main purpose of this flow meter is to measure the flow rate of working fluid.

A U-tube manometer with measurement capacity of (0–140 mmHg) having an accuracy of ±1 mmHg is used. The 1<sup>st</sup> tube end of manometer is joined with the main fluid line, which is connected to the automobile radiator i.e. radiator inlet fluid line. The 2<sup>nd</sup> tube end of manometer is joined with the radiator outlet fluid line, which is connected to the storage tank. The both connections of manometer tube are made with the help of silicone rubber tubes having a diameter of 7.35 mm. The main purpose of this manometer is to calculate the fluid pressure drop across the automobile radiator by taking measurement of its fluid (mercury) height. Twelve type K thermocouples with digital display temperature controller (REX-C100) having an accuracy of ±0.2°C are used. Its measurement capacity is (0–400°C). The 1<sup>st</sup> one is placed on the radiator inlet fluid line and 2<sup>nd</sup> one is placed on the radiator outlet fluid line. The main purpose of these two thermocouples is to measure the fluid temperature across

the automobile radiator. The 3<sup>rd</sup> one is placed on the fluid storage tank in order to measure the temperature of working fluid. The remaining nine thermocouples are placed on the outer side wall of automobile radiator at different positions. The main purpose of these nine thermocouples is to measure the mean wall temperature of automobile radiator. When working fluid is heated up at desired temperature, then it is passed through the automobile radiator with the help of centrifugal pump.

The power supply (AC) is used to run the experimental setup. A simple control panel is used to control the components of experimental setup. It consists of main power supply on/off switch, centrifugal pump on/off switch, radiator fan on/off switch, electric heater on/off switch and digital temperature controller display screens. All the instruments used in this experimental setup are fully-calibrated by the manufacturer's certifications. The detailed list of these instruments is given in Table 3.

**Table 3** Detailed list of instruments used in the experimental setup

Instrument	Quantity, type and accuracy
Thermocouples	12, K-type, accuracy ±0.2°C
Flow meter (Rotameter)	1, LZT-1005M, accuracy ±4% reading
Manometer	1, U-tube-type, accuracy ±1 mmHg
Power supply (AC)	220–240 V, 50/60 Hz
Electric water heater	1, R-T-M-type, 1500 W
Heater thermostat (single-pole)	1, Stem-type, accuracy ±1°C
Centrifugal pump (single-stage)	1, VALCO-55CG, 370 W
Ball valve (Drain valve)	1
Gate valves	2
Storage tank	1, Capacity 40 liters
Automobile radiator	1, 33 flattened aluminium tubes
Electric fan (DC)	1, 12 V, 800 – 900 r/min
Control panel	1
Supporting stand	1

First of all, power supply (AC) was provided to the experimental setup. After that, storage tank was filled with the working fluid having a total volume of 20 liters, which was to be investigated. Then heater switch was put “on” for heating the working fluid at desired temperature. This desired temperature of working fluid was set with the help of heater thermostat. When working fluid was heated up at required temperature then centrifugal pump switch was put “on” and the fluid flow rate was adjusted at desired level with the help of gate valves. This desired flow rate of working fluid was then passed through the automobile radiator via flow meter with the help of centrifugal pump. After that, radiator fan switch was put

“on” in order to transfer the heat energy from working fluid to the atmosphere. At that moment, fluid temperature across the automobile radiator and radiator wall temperatures were measured with the help of thermocouples. Furthermore, corresponding manometer fluid (mercury) height was measured with the help of millimeter scale ruler, which was placed on the frame of manometer. At last, the desired parameters like heat transfer rate, overall heat transfer coefficient, Nusselt number, Reynolds number and other factors like pressure drop and friction factor of working fluid across the automobile radiator were calculated by using these temperature and manometer fluid (mercury) height readings. All the experiments were performed at constant fluid volume flow rates (2, 4, 6, 8, 10, 12 L/min) by using pure water and ZnO water nanofluids with 0.1%, 0.2% and 0.3% volumetric concentrations as working fluids at constant fluid inlet temperature to the automobile radiator ((70±1) °C) and steady state reading was obtained after time interval of 4–5 minutes.

### 2.3 Data reduction

In this research work, the correlations proposed by various scientists [18–21], have been utilized to calculate the density, specific heat, viscosity and thermal conductivity of nanofluids respectively at various temperatures and volumetric concentrations of nanoparticles as given by Eqs. (1) – (4):

$$\rho_{nf} = \phi\rho_p + (1-\phi)\rho_w \quad (1)$$

$$(\rho C_p)_{nf} = \phi(\rho C_p)_p + (1-\phi)(\rho C_p)_w \quad (2)$$

$$\mu_{nf} = (1 + 7.3\phi + 123\phi^2)\mu_w \quad (3)$$

$$k_{nf} = \frac{k_p + 2k_w + 2(k_p - k_w)\phi}{k_p + 2k_w - (k_p - k_w)\phi} k_w \quad (4)$$

where  $\rho_{nf}$ ,  $C_{pnf}$ ,  $\mu_{nf}$  and  $k_{nf}$  are known as density, specific heat, viscosity and thermal conductivity of nanofluid;  $\phi$  stands for volumetric concentration of nanoparticles;  $\rho_p$ ,  $C_{pp}$  and  $k_p$  are the density, specific heat and thermal conductivity of nanoparticles and  $\rho_w$ ,  $C_{pw}$ ,  $\mu_w$  and  $k_w$  are the density, specific heat, viscosity and thermal conductivity of water, respectively.

Heat transfer rate can be determined by using Eq. (5):

$$Q = \dot{m}C_p(T_{in} - T_{out}) \quad (5)$$

where  $Q$  is known as heat transfer rate;  $C_p$  stands for specific heat of fluid;  $T_{in}$  and  $T_{out}$  are the fluid inlet and outlet temperature to the automobile radiator and  $\dot{m}$  is the mass flow rate of fluid calculated by using Eq. (6):

$$\dot{m} = \rho\dot{V} \quad (6)$$

where  $\rho$  is the density of fluid and  $\dot{V}$  is the volumetric flow rate of fluid.

Heat transfer coefficient can be determined by using Eq. (7):

$$h = \frac{Q}{nA_s(T_b - T_{wa})} \quad (7)$$

where  $h$  is known as heat transfer coefficient;  $Q$  stands for heat transfer rate;  $n$  stands for number of radiator tubes;  $A_s$  stands for surface area of radiator tube and  $T_b$  is the mean temperature of fluid inlet and outlet temperature called bulk temperature calculated by Eq. (8):

$$T_b = \frac{T_{in} + T_{out}}{2} \quad (8)$$

where  $T_{in}$  is the fluid inlet temperature and  $T_{out}$  is the fluid outlet temperature. The  $T_{wa}$  is the mean wall temperature of automobile radiator calculated by Eq. (9):

$$T_{wa} = \frac{T_1 + T_2 + \dots + T_8 + T_9}{9} \quad (9)$$

where  $T_1, T_2, \dots, T_8$  and  $T_9$  are the wall temperatures of automobile radiator at different positions, respectively.

Overall heat transfer coefficient can be calculated by using Eq. (10):

$$U = \frac{Q}{nA_s(LMTD)} \quad (10)$$

where  $U$  is known as overall heat transfer coefficient;  $Q$  stands for heat transfer rate;  $n$  stands for number of radiator tubes;  $A_s$  stands for radiator tube surface area and  $LMTD$  is the logarithmic mean temperature difference calculated by using Eq. (11):

$$LMTD = \frac{T_{in} - T_{out}}{\ln \frac{T_{in}}{T_{out}}} \quad (11)$$

where  $T_{in}$  is the fluid inlet temperature and  $T_{out}$  is the fluid outlet temperature.

Pressure drop can be calculated by using Eq. (12):

$$\Delta P = (\rho_{Hg} - \rho)g\Delta h \quad (12)$$

where  $\Delta P$  is known as pressure drop or pressure difference;  $\rho_{Hg}$  stands for manometer fluid (mercury) density;  $g$  stands for gravitational acceleration;  $\rho$  stands for density of fluid and  $\Delta h$  is the manometer reading, which is obtained due to the height difference of manometer fluid (mercury).

Friction factor depends upon pressure drop, which can be determined by using Eq. (13):

$$f = \frac{2\Delta P}{n(L/d_H)\rho v^2} \quad (13)$$

where  $f$  is known as friction factor;  $\Delta P$  stands for pressure drop;  $n$  stands for number of radiator tubes;  $L$  stands for length of radiator tube;  $d_H$  stands for hydraulic diameter of radiator tube;  $\rho$  stands for density of fluid and  $v$  is the flow velocity of fluid calculated by Eq. (14):

$$v = \frac{\dot{V}}{nA_c} \quad (14)$$

where  $\dot{V}$  is known as volumetric flow rate of fluid;  $n$  stands for number of radiator tubes and  $A_c$  is the cross sectional area of radiator tube.

Pumping power also depends upon pressure drop, which can be calculated by using Eq. (15):

$$W_p = \dot{V}\Delta P \quad (15)$$

where  $W_p$  is known as pumping power;  $\Delta P$  stands for pressure drop and  $\dot{V}$  is the volumetric flow rate of fluid.

Reynolds number can be calculated by using famous Eq. (16):

$$Re = \frac{\rho v d_H}{\mu} \quad (16)$$

where  $Re$  is known as Reynolds number;  $\rho$  stands for fluid density;  $v$  stands for fluid flow velocity;  $d_H$  stands for hydraulic diameter of radiator tube and  $\mu$  is the fluid viscosity.

Nusselt number can be determined by using Eq. (17):

$$Nu = \frac{h d_H}{k} \quad (17)$$

where  $Nu$  is known as Nusselt number;  $h$  stands for heat transfer coefficient;  $d_H$  stands for hydraulic diameter of radiator tube and  $k$  is the fluid thermal conductivity.

Prandtl number can be determined by using Eq. (18):

$$Pr = \frac{\mu C_p}{k} \quad (18)$$

where  $Pr$  is known as Prandtl number;  $\mu$  stands for fluid viscosity;  $C_p$  stands for fluid specific heat and  $k$  is the fluid thermal conductivity.

Since the radiator tubes have elliptical cross section as shown in Fig. 2, their cross sectional area can be calculated by using Eq. (19):

$$A_c = \frac{\pi}{4} d^2 + (D-d)d \quad (19)$$

where  $A_c$  is known as radiator tube cross sectional area;  $D$  stands for major diameter of radiator tube and  $d$  is the minor diameter of radiator tube.

Similarly, surface area of radiator tube can be calculated by using Eq. (20):

$$A_s = PL \quad (20)$$

where  $A_s$  is known as radiator tube surface area;  $P$  stands for perimeter of radiator tube and  $L$  is the length of radiator tube.

Hydraulic diameter of radiator tube can be determined by using Eq. (21):

$$d_H = \frac{4A_c}{P} \quad (21)$$

where  $d_H$  is known as hydraulic diameter of radiator tube;

$A_c$  stands for radiator tube cross sectional area and  $P$  is the perimeter of radiator tube calculated by Eq. (22):

$$P = \pi d + 2(D-d) \quad (22)$$

where  $D$  is the major diameter of radiator tube and  $d$  is the minor diameter of radiator tube.

## 2.4 Uncertainty analysis

The uncertainty analysis was done by estimating the measurement errors of experimental data. The uncertainty in Nusselt number takes place due to the measurement errors of fluid volume flow rate, all the radiator tube dimensions like its length and both diameters and all the temperature values including radiator inlet and outlet fluid temperature and its wall temperatures. Similarly, the uncertainty in overall heat transfer coefficient occurs due to the measurement errors of all above input parameters except radiator wall temperatures, while the uncertainty in heat transfer rate happens due to the measurement errors of fluid volume flow rate and radiator inlet and outlet fluid temperature.

On the other side, the uncertainty in friction factor occurs due to the measurement errors of manometer fluid (mercury) height, fluid volume flow rate and all the radiator tube dimensions like its length and both diameters, while the uncertainty in pressure drop happens only due to the measurement error of manometer fluid (mercury) height. Similarly, the uncertainty in pumping power takes place due to the measurement errors of fluid volume flow rate and manometer fluid (mercury) height. Furthermore, the uncertainty in Reynolds number occurs due to the measurement errors of fluid volume flow rate and both diameters of radiator tube, while the uncertainty in hydraulic diameter happens only due to the measurement error of both diameters of radiator tube.

In this experimental work, the uncertainties in all desired parameters were calculated by utilizing the technique, which was proposed by Holman [22] and all these uncertainties are given in Table 4. Moreover, a few experiments were performed again in order to examine the reproducibility of experimentation later on, whose results were confirmed to be perfect.

**Table 4** Uncertainties in all desired parameters

Parameter	Range of values	Uncertainties/%
$Nu$	4.21–8.14	4.23
$U$	70–172 W/(m <sup>2</sup> ·K)	3.43
$Q$	2369–6265 W	4
$f$	0.09–0.63	16.20
$\Delta P$	184.12–3188 Pa	24
$W_p$	6.26–650.35 mW	28.96
$Re$	186–1127	4.18
$d_H$	3.7632 mm	0.47

### 3. Results and Discussions

#### 3.1 Validation of experimental setup

The reliability and accuracy of experimental setup were examined before calculating the desired parameters of nanofluids like heat transfer rate, overall heat transfer

$$Nu = 1.953 \left( RePr \frac{d_H}{L} \right)^{\frac{1}{3}} \quad \text{for} \left( RePr \frac{d_H}{L} \right) \geq 33.33 \tag{23}$$

$$Nu = 4.364 + 0.0722 \left( RePr \frac{d_H}{L} \right) \quad \text{for} \left( RePr \frac{d_H}{L} \right) \leq 33.33$$

$$Nu = 1.9421 \left( RePr \frac{d_H}{L} \right)^{0.3} \quad \text{for} \left( RePr \frac{d_H}{L} \right) \geq 33.33 \tag{24}$$

$$Nu = 6.1 + 0.003675 \left( RePr \frac{d_H}{L} \right) \quad \text{for} \left( RePr \frac{d_H}{L} \right) \leq 33.33$$

Similarly, experimental outcomes of friction factor were compared with the expected values acquired from the Darcy-Weisbach [25] correlation for laminar flow, as given by Eq. (25):

$$f = \frac{64}{Re} \tag{25}$$

The comparison between current experimental work and existing Nusselt number correlations for pure water at laminar flow is illustrated in Fig. 3. From Fig. 3, it can be clearly seen that the experimental outcomes of Nusselt number for pure water exhibit a good agreement with Shah-London [23] correlation having a mean error of 4.89% at given range of Reynolds number i.e.  $186 \leq Re \leq 1127$ , while Vajjha [24] correlation exhibits a disagreement with this experimental work due to high mean error of 32.85%.

Similarly, the comparison between current experimental work and existing friction factor correlation for pure water at laminar flow is illustrated in Fig. 4. From Fig. 4, it can be clearly seen that the experimental

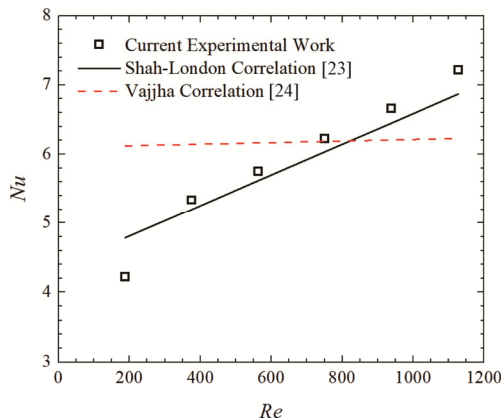


Fig. 3 Comparison between current experimental work and existing correlations for Nusselt number

coefficient, Nusselt number, pressure drop and friction factor etc. This was taken by utilizing water as working liquid. The experimental outcomes of Nusselt number were compared with the expected values acquired from the Shah-London [23] and Vajjha [24] correlations for laminar flow, as given by Eqs. (23)–(24):

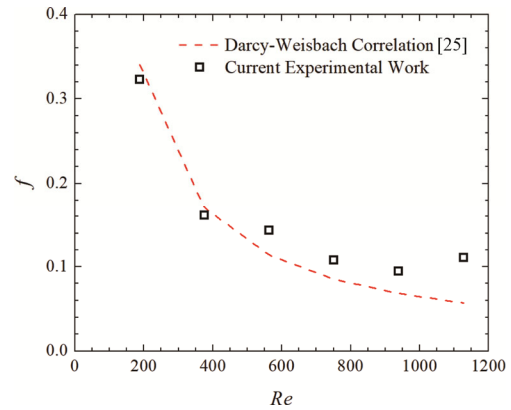


Fig. 4 Comparison between current experimental work and existing correlation for friction factor

outcomes of friction factor for pure water exhibit a good agreement with Darcy-Weisbach [25] correlation having a mean error of 15.20% at given range of Reynolds number i.e.  $186 \leq Re \leq 1127$ .

#### 3.2 Thermal performance parameters of ZnO water nanofluids

##### 3.2.1 Heat transfer rate

The graphical representation of heat transfer rates vs. volume flow rates for pure water and ZnO water nanofluids with 0.1%, 0.2% and 0.3% volumetric concentrations of nanoparticles is illustrated in Fig. 5. The heat transfer rates of pure water are taken as reference values in order to predict the heat transfer augmentation of nanofluids. From Fig. 5, it can be clearly observed that the heat transfer rate increases by increasing the volume flow rate of pure water as well as ZnO water nanofluids. However, heat transfer rates of nanofluids are higher as compared to pure water.



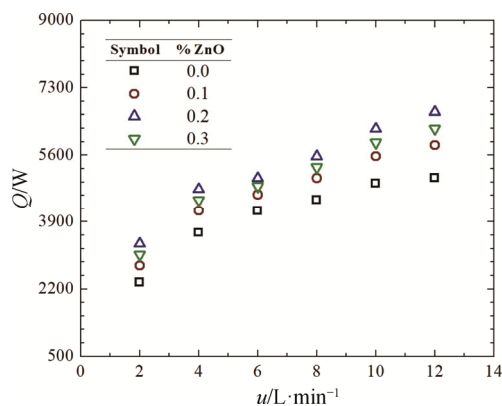


**Fig. 5** Heat transfer rate vs. volume flow rate for pure water and ZnO water nanofluids

In the case of pure water, value of heat transfer rate is 2369 W at 2 L/min and 5016 W at 12 L/min for this current work. Various volumetric concentrations of nanoparticles have shown various heat transfer enhancements at various volume flow rates, when it is compared to pure water, e.g. ZnO water nanofluids with 0.2% and 0.3% volumetric concentrations show maximum heat transfer enhancements at 2 L/min. The heat transfer rates of ZnO water nanofluid with 0.1% volumetric concentration are 9.96%–17.61% higher as compared to pure water. From Fig. 5, it can also be clearly observed that the heat transfer rate increases by increasing the volumetric concentration of nanoparticles. However, this enhancement in heat transfer is limited up to certain nanoparticles volumetric concentration level i.e. 0.2% volumetric concentration. It can also be observed that the influence of ZnO water nanofluid with 0.2% volumetric concentration on heat transfer enhancement is highly appreciable.

From Fig. 5, it can also be clearly observed that the heat transfer rates start to decline when volumetric concentration of nanoparticles is increased from 0.2% to 0.3%. The reason behind this is that the density and viscosity of nanofluid increases by increasing the volumetric concentration of nanoparticles, e.g. an increase of 0.1% in nanoparticles volumetric concentration yields about 1% increase in density and viscosity of nanofluid. So, this increase in density and viscosity of nanofluid results into high wall shear stress that leads to a denser boundary layer inside the radiator tube. Hence, according to this phenomenon, the rate of heat transfer may be decreased [2,4,17,26].

### 3.2.2 Heat transfer enhancement

The graphical representation of heat transfer enhancements of ZnO water nanofluids vs. volumetric concentrations of nanoparticles at various volume flow rates are illustrated in Fig. 6. From Fig. 6, it can be clearly observed that the heat transfer rates are increased

by using ZnO water nanofluids with 0.1%, 0.2% and 0.3% volumetric concentrations, when it is compared to pure water.

From Fig. 6, it can be clearly observed that the high values of heat transfer enhancements are observed at low volume flow rate (2 L/min) as compared to high volume flow rate (12 L/min). For instance, ZnO water nanofluids with 0.2% and 0.3% volumetric concentrations show 41.08% and 29.29% heat transfer enhancements at 2 L/min as compared to pure water respectively. However, ZnO water nanofluids with 0.2% and 0.3% volumetric concentrations show 19.92% and 14.89% heat transfer enhancements at 12 L/min as compared to pure water respectively. Hence, ZnO water nanofluid with 0.2% volumetric concentration shows maximum heat transfer enhancement i.e. 41.08% at 2 L/min.

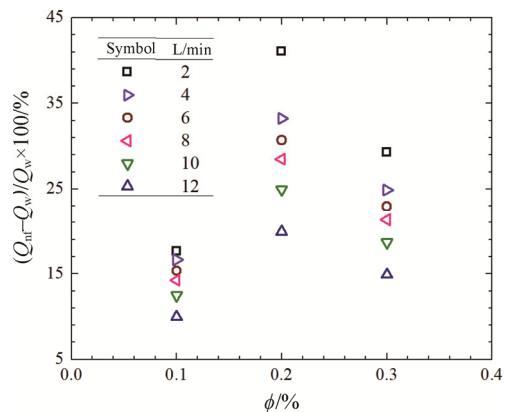


**Fig. 6** Heat transfer enhancement vs. volumetric concentration of ZnO nanoparticles in nanofluids at various volume flow rates

The heat transfer enhancements are obtained due to the excellent thermal properties of ZnO water nanofluids, like low specific heat and high thermal conductivity as compared to pure water [4, 8]. Since nanofluids have low specific heat and high thermal conductivity due to the suspended ZnO nanoparticles, they absorb smaller amount of heat in order to get the particular temperature i.e. heat up quickly as compared to pure water [13, 15]. Furthermore, nanofluids have high specific surface area due to the suspended ZnO nanoparticles, therefore, they extract greater amount of heat in order to lose the particular temperature i.e. cool down quickly as compared to pure water. Moreover, flow pattern, dispersion, fluctuation, Brownian movement and migration of suspended ZnO nanoparticles play a significant role in the heat transfer of nanofluids, because these factors will further boost up the heat transfer ability of ZnO nanoparticles. Hence, according to these facts, the heat transfer rates of ZnO water nanofluids are higher as compared to pure water [27, 17, 28–31].

### 3.2.3 Overall heat transfer coefficient

The graphical representation of overall heat transfer coefficients vs. volume flow rates for pure water and ZnO water nanofluids with 0.1%, 0.2% and 0.3% volumetric concentrations of nanoparticles are illustrated in Fig. 7. From Fig. 7, it can be clearly observed that the overall heat transfer coefficient increases by increasing the volume flow rate of pure water as well as ZnO water nanofluids, which is similar to the case of heat transfer rate. However, overall heat transfer coefficients of nanofluids are higher as compared to pure water.

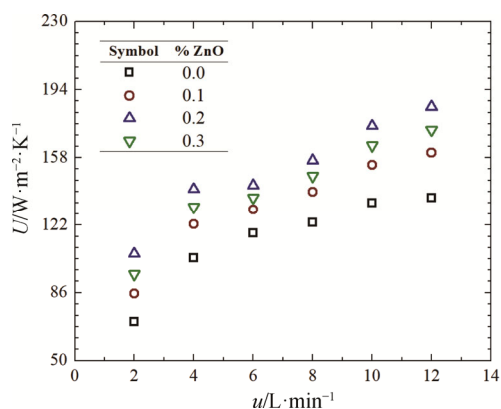


Fig. 7 Overall heat transfer coefficient vs. volume flow rate for pure water and ZnO water nanofluids

From Fig. 7, it can also be clearly observed that the overall heat transfer coefficient increases by increasing the volumetric concentration of nanoparticles. However, this enhancement in overall heat transfer coefficient is limited up to certain nanoparticles volumetric concentration level, which is also similar to the case of heat transfer rate i.e. 0.2% volumetric concentration. From Fig. 7, it can also be clearly observed that the overall heat transfer coefficients start to decline when volumetric concentration of nanoparticles is increased from 0.2% to 0.3%. The reason behind this is explained briefly in the section of heat transfer rate.

In the case of pure water, value of overall heat transfer coefficient is 70 W/(m<sup>2</sup>·K) at 2 L/min and 136 W/(m<sup>2</sup>·K) at 12 L/min for this current work. The ZnO water nanofluids with various volumetric concentrations of nanoparticles have shown various enhancements in overall heat transfer coefficient at various volume flow rates, when it is compared to pure water. The overall heat transfer coefficients of ZnO water nanofluid with 0.1% volumetric concentration are 10.86%–20.90% higher as compared to pure water. The ZnO water nanofluids with 0.2% and 0.3% volumetric concentrations show 50.82% and 35.49% enhancements in overall heat transfer coefficient at 2 L/min as compared to pure water respectively. However, ZnO water nanofluids with 0.2%

and 0.3% volumetric concentrations show 35.34% and 26.34% enhancements in overall heat transfer coefficient at 12 L/min as compared to pure water, respectively. Hence, ZnO water nanofluid with 0.2% volumetric concentration shows maximum enhancement in overall heat transfer coefficient i.e. 50.82% at 2 L/min.

### 3.2.4 Nusselt number

The graphical representation of values of Nusselt number vs. values of Reynolds number for pure water and ZnO water nanofluids with 0.1%, 0.2% and 0.3% volumetric concentrations of nanoparticles are illustrated in Fig. 8. From Fig. 8, it can be clearly observed that the Nusselt number increases by increasing the Reynolds number of pure water as well as ZnO water nanofluids. However, Nusselt number values of nanofluids are higher as compared to pure water.

The Reynolds number is highly dependent on the radiator tube geometry, flow velocity, density and viscosity of working fluid that flows in the tubes of radiator. Since velocity increases by increasing the volume flow rate, Reynolds number is increased by increasing the volume flow rate of all working fluids i.e. pure water and ZnO water nanofluids. From Fig. 8, it can also be clearly observed that the Nusselt number increases by increasing the volumetric concentration of nanoparticles. However, this enhancement in Nusselt number is limited up to certain nanoparticles volumetric concentration level, which is also similar to the case of heat transfer rate i.e. 0.2% volumetric concentration. From Fig. 8, it can also be clearly observed that the values of Nusselt number start to decline when volumetric concentration of nanoparticles is increased from 0.2% to 0.3%. The reason behind this is also explained briefly in the section of heat transfer rate.

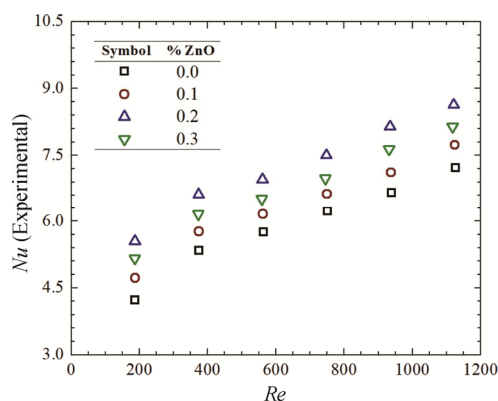


Fig. 8 Nusselt number vs. Reynolds number for pure water and ZnO water nanofluids

In the case of pure water, value of Nusselt number is 4.21 at Re=187 and 7.21 at Re=1127 for this current work. The ZnO water nanofluids with various volumetric concentrations of nanoparticles have shown various

enhancements in Nusselt number at various values of Reynolds number, when it is compared to pure water. The Nusselt number values of ZnO water nanofluid with 0.1% volumetric concentration are 6.56%–11.93% higher as compared to pure water. The ZnO water nanofluids with 0.2% and 0.3% volumetric concentrations show 31.49% and 22.33% enhancements in Nusselt number at  $Re=186$  as compared to pure water respectively. However, ZnO water nanofluids with 0.2% and 0.3% volumetric concentrations show 19.58% and 12.92% enhancements in Nusselt number at  $Re=1121$ , and 1117 as compared to pure water respectively. Hence, ZnO water nanofluid with 0.2% volumetric concentration shows maximum enhancement in Nusselt number i.e. 31.49% at  $Re=186$ .

### 3.3 Pressure drop and friction factor of ZnO water nanofluids

It is very important to estimate the pressure drop and friction factor of nanofluid along with the thermal performance before applying the nanofluids in automobile and industrial cooling systems.

#### 3.3.1 Pressure drop

The graphical representation of values of pressure drop vs. values of Reynolds number for pure water and ZnO water nanofluids with 0.1%, 0.2% and 0.3% volumetric concentrations of nanoparticles at radiator inlet temperature of 70°C is illustrated in Fig. 9. The pressure drop values of pure water are taken as reference values in order to predict the enhancement in pressure drop of nanofluids. From Fig. 9, it can be clearly observed that the pressure drop increases by increasing the Reynolds number of pure water as well as ZnO water nanofluids. However, pressure drop values of nanofluids are higher as compared to pure water.

From Fig. 9, it can also be clearly observed that the pressure drop increases by increasing the volumetric concentration of nanoparticles. In the case of pure water, value of pressure drop is 184.12 Pa at  $Re=187$  and

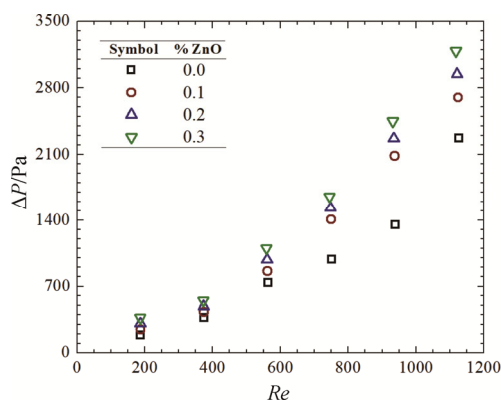


**Fig. 9** Pressure drop vs. Reynolds number for pure water and ZnO water nanofluids

2270.89 Pa at  $Re=1127$  for this current work. The ZnO water nanofluids with various volumetric concentrations of nanoparticles have shown various enhancements in pressure drop at various values of Reynolds number, when it is compared to pure water. The pressure drop values of ZnO water nanofluid with 0.1% volumetric concentration are 16.62%–54.48% higher as compared to pure water. The ZnO water nanofluids with 0.2% and 0.3% volumetric concentrations show 66.54% and 99.77% enhancements in pressure drop at  $Re=186$  as compared to pure water respectively. However, ZnO water nanofluids with 0.2% and 0.3% volumetric concentrations show 29.63% and 40.38% enhancements in pressure drop at  $Re=1121$ , and 1117 as compared to pure water respectively. Moreover, mean enhancements in pressure drop of ZnO water nanofluids with 0.1%, 0.2% and 0.3% volumetric concentrations are 30.59%, 47.80% and 65.00% respectively, when it is compared to pure water.

The enhancements in pressure drop are obtained due to the inferior physical properties of ZnO water nanofluids, like high density and viscosity as compared to pure water [6, 16]. Since nanofluids have high density and viscosity due to the suspended ZnO nanoparticles, they possess more friction during flowing in a channel i.e. high flow resistant as compared to pure water. Furthermore, flow pattern, dispersion, fluctuation, Brownian movement and migration of suspended ZnO nanoparticles also play a significant role in the pressure drop of nanofluids, because these factors further boost up the rates of momentum transfer among the ZnO nanoparticles, and this momentum transfer significantly enhances the pressure drop. Hence, according to these facts, the pressure drop values of ZnO water nanofluids are higher as compared to pure water [32].

#### 3.3.2 Friction factor

The graphical representation of values of friction factor vs. values of Reynolds number for pure water and ZnO water nanofluids with 0.1%, 0.2% and 0.3% volumetric concentrations of nanoparticles at radiator inlet temperature of 70°C is illustrated in Fig. 10. From Fig. 10, it can be clearly observed that the friction factor decreases by increasing the Reynolds number of pure water as well as ZnO water nanofluids. However, friction factor values of nanofluids are higher as compared to pure water.

From Fig. 10, it can also be clearly observed that the friction factor increases by increasing the volumetric concentration of nanoparticles. In the case of pure water, value of friction factor is 0.32 at  $Re=187$  and 0.11 at  $Re=1127$  for this current work. The ZnO water nanofluids with various volumetric concentrations of nanoparticles have shown various enhancements in friction factor at various values of Reynolds number, when it is compared

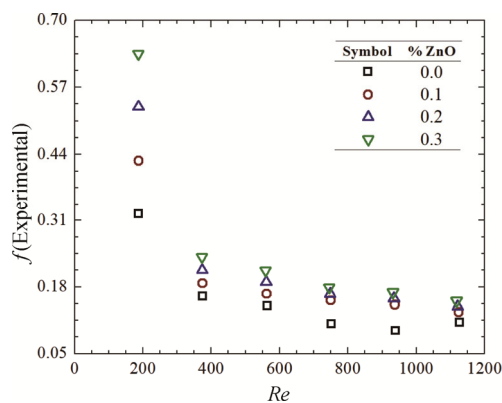


**Fig. 10** Friction factor vs. Reynolds number for pure water and ZnO water nanofluids

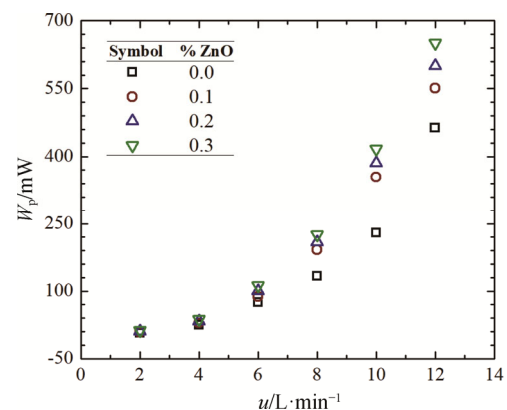


**Fig. 11** Pumping power vs. volume flow rate for pure water and ZnO water nanofluids

to pure water. The friction factor values of ZnO water nanofluid with 0.1% volumetric concentration are 16.07–53.76% higher as compared to pure water. The ZnO water nanofluids with 0.2% and 0.3% volumetric concentrations show 64.98% and 96.98% enhancements in friction factor at  $Re=186$  as compared to pure water respectively. However, ZnO water nanofluids with 0.2% and 0.3% volumetric concentrations show 28.41% and 38.41% enhancements in friction factor at  $Re=1121, 1117$  as compared to pure water respectively. Moreover, mean enhancements in friction factor of ZnO water nanofluids with 0.1%, 0.2% and 0.3% volumetric concentrations are 29.98%, 46.42% and 62.69% respectively, when it is compared to pure water.

The friction factor is strongly dependent on the pressure drop, radiator tube geometry, flow velocity, density and viscosity of working fluid that flows in the tubes of radiator. Therefore, the facts according to which friction factor values of ZnO water nanofluids are higher as compared to pure water, are the same as in the case of pressure drop, and these facts are briefly discussed in the section of pressure drop.

### 3.4 Pumping power for ZnO water nanofluids

The graphical representation of values of pumping power vs. volume flow rates for pure water and ZnO water nanofluids with 0.1%, 0.2% and 0.3% volumetric concentrations of nanoparticles at radiator inlet temperature of 70°C is illustrated in Fig. 11. The pumping power values for pure water are taken as reference values in order to predict the enhancement in pumping power for nanofluids. From Fig. 11, it can be clearly observed that the pumping power increases by increasing the volume flow rate of pure water as well as ZnO water nanofluids. However, pumping power values for nanofluids are higher as compared to pure water.

From Fig. 11, it can also be clearly observed that the pumping power increases by increasing the volumetric

concentration of nanoparticles. In the case of pure water, value of pumping power is 6.26 mW at 2 L/min and 463.26 mW at 12 L/min for this current work. The ZnO water nanofluids with various volumetric concentrations of nanoparticles have shown various enhancements in pumping power at various volume flow rates, when it is compared to pure water. The pumping power values for ZnO water nanofluid with 0.1% volumetric concentration are 16.62%–54.48% higher as compared to pure water. The ZnO water nanofluids with 0.2% and 0.3% volumetric concentrations show 66.54% and 99.77% enhancements in pumping power at 12 L/min as compared to pure water respectively. However, ZnO water nanofluids with 0.2% and 0.3% volumetric concentrations show 29.63% and 40.38% enhancements in pumping power at 12 L/min as compared to pure water, respectively. Moreover, mean enhancements in pumping power for ZnO water nanofluids with 0.1%, 0.2% and 0.3% volumetric concentrations are 30.59%, 47.80% and 65.00% respectively, when it is compared to pure water.

The pumping power is also strongly dependent on the pressure drop and volume flow rate of working fluid that flows in the tubes of radiator. Therefore, the facts according to which pumping power values for ZnO water nanofluids are higher as compared to pure water, are the same as in the case of pressure drop, and these facts are briefly discussed in the section of pressure drop. Thus, additional pumping power is required whenever nanofluids with high volumetric concentrations of nanoparticles are going to be used at low or high volume flow rates in any type of industrial cooling systems [17,27,33,32].

### 3.5 Radiator efficiency using ZnO water nanofluids

In practical point of view for all cooling systems at the same volume flow rate, it is also very important to describe that the more decrement in the temperature of working fluid indicates an ideal thermal efficiency of a



cooling system. Therefore, graphical representation of radiator outlet temperatures vs. volume flow rates for pure water and ZnO water nanofluids with 0.1%, 0.2% and 0.3% volumetric concentrations of nanoparticles at radiator inlet temperature of 70°C is illustrated in Fig. 12.

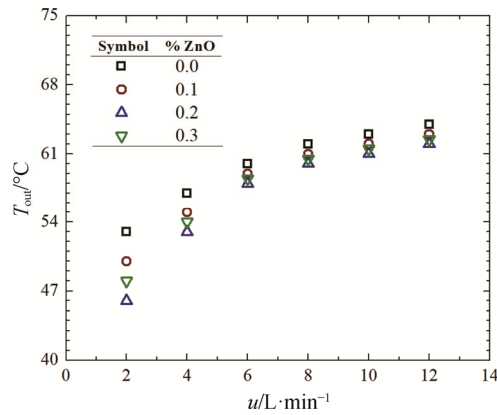


**Fig. 12** Radiator outlet temperature vs. volume flow rate for pure water and ZnO water nanofluids

From Fig. 12, it can be clearly observed that the outlet temperatures of radiator are decreased by using ZnO water nanofluids with 0.1%, 0.2% and 0.3% volumetric concentrations, when it is compared to pure water. This shows that the thermal efficiency of radiator is improved by using ZnO water nanofluids with 0.1%, 0.2% and 0.3% volumetric concentrations as compared to pure water. From Fig. 12, it can also be clearly observed that the heat transfer rate of radiator is decreased by increasing the volume flow rate of all working fluids i.e. pure water and ZnO water nanofluids. The reason behind this is that the velocity of working fluid increases by increasing the volume flow rate, therefore working fluid has a short time to stay within the tubes of radiator and contact with the cold air, which is supplied by the radiator fan. As a result, outlet temperatures of radiator are enhanced [7,14,33]. Hence, maximum thermal efficiency of radiator with high heat transfer rates is achieved by using ZnO water nanofluid with 0.2% volumetric concentration as compared to pure water.

#### 4. Conclusions

The most effective results have been achieved from this research work and are described as following:

Remarkable enhancements in the thermal performance parameters like heat transfer rate, overall heat transfer coefficient and Nusselt number have been recorded by utilizing ZnO water nanofluids, when it is compared to pure water. For instance, the maximum enhancement in heat transfer rate is obtained up to 41% by using nanofluid with 0.2% volumetric concentration of nanoparticles. Likewise, the maximum enhancement in

overall heat transfer coefficient and Nusselt number is also obtained up to 50% and 31% by using nanofluid with same volumetric concentration of nanoparticles i.e. 0.2% respectively. Furthermore, considerable enhancements in pressure drop and friction factor of ZnO water nanofluids along with magnificent thermal performance have been also observed, when it is compared to pure water. For instance, the mean enhancement in pressure drop and friction factor is obtained up to 47% and 46% by using nanofluid with 0.2% volumetric concentration of nanoparticles, respectively. Thus, a minor penalty in term of extra pumping power is to be faced whenever nanofluids with high volumetric concentrations of nanoparticles are going to implement in any kind of industrial thermal applications.

The experimental outcomes reveal that the thermal performance as well as pressure drop and friction factor of nanofluids is strongly reliant on the volume flow rate and volumetric concentration of nanoparticles. Therefore, heat transfer rate, overall heat transfer coefficient and Nusselt number of nanofluids increases by increasing the volume flow rate and volumetric concentration of nanoparticles. However, this increment in these thermal performance parameters is limited up to certain nanoparticles volumetric concentration level i.e. 0.2% volumetric concentration. This means that the heat transfer rate, overall heat transfer coefficient and Nusselt number of nanofluids start to decline when volumetric concentration of nanoparticles is increased from 0.2% to 0.3%. Furthermore, pressure drop and friction factor of nanofluids increases by increasing the volumetric concentration of nanoparticles, while pressure drop increases and friction factor decreases by increasing the volume flow rate of nanofluids respectively. Moreover, the thermal efficiency of automobile radiator is improved by utilizing ZnO water nanofluids, when it is compared to pure water. For example, the magnificent thermal efficiency of automobile radiator with high heat transfer rates is obtained by using nanofluid with 0.2% volumetric concentration of nanoparticles.

Hence, in the light of all above results, the magnificent thermal performance is achieved by utilizing ZnO water nanofluids as compared to pure water, which indicates that the nanofluids have a bright future in automobile and heat exchanger manufacturing companies. This superior heat transfer enhancement of nanofluids may result into compact and lightweight automobile radiators, which leads to improve the automobile engine performance with low fuel consumption.

#### Acknowledgement

The authors are thankful to University of Engineering and Technology, Lahore, Pakistan for providing resources

for this work and Higher Education Commission, Islamabad, Pakistan for providing financial support [Grant No. 21-2245/SRGP/HRD/HEC/2018].

## References

- [1] Ali H.M., Azhar M.D., Saleem M., Saeed Q.S., Saieed A., Heat transfer enhancement of car radiator using aqua based magnesium oxide nanofluids. *Thermal Science* 2015, 19(6): 2039–2048.
- [2] Ali H.M., Ali H., Liaquat H., Maqsood H.T.B., Nadir M.A., Experimental investigation of convective heat transfer augmentation for car radiator using ZnO–water nanofluids. *Energy*, 2015, 84: 317–324.
- [3] Bhogare A.R.A., Kothawale B., Bodkhe P.P., Gawali A., Performance investigation of Automobile Radiator operated with Nanofluids Based Coolant. *International Journal of Thermal Technologies*, 2014, 4(2): 2277–4114.
- [4] Ali M., El-Leathy A., Al-Sofyany Z., The effect of nanofluid concentration on the cooling system of vehicles radiator. *Advances in Mechanical Engineering*, 2014, 6: 962510.
- [5] Heris S.Z., Pour M.B., Mahian O., Wongwises S., A comparative experimental study on the natural convection heat transfer of different metal oxide nanopowders suspended in turbine oil inside an inclined cavity. *International Journal of Heat and Mass Transfer*, 2014, 73: 231–238.
- [6] Leong K., Saidur R., Kazi S., Mamun A., Performance investigation of an automotive car radiator operated with nanofluid-based coolants (nanofluid as a coolant in a radiator). *Applied Thermal Engineering*, 2010, 30 (17–18): 2685–2692.
- [7] Peyghambarzadeh S., Hashemabadi S., Jamnani M.S., Hoseini S., Improving the cooling performance of automobile radiator with Al<sub>2</sub>O<sub>3</sub>/water nanofluid. *Applied Thermal Engineering*, 2011, 31(10): 1833–1838.
- [8] Peyghambarzadeh S., Hashemabadi S., Naraki M., Vermahmoudi Y., Experimental study of overall heat transfer coefficient in the application of dilute nanofluids in the car radiator. *Applied Thermal Engineering*, 2013, 52(1): 8–16.
- [9] Naraki M., Peyghambarzadeh S., Hashemabadi S., Vermahmoudi Y., Parametric study of overall heat transfer coefficient of CuO/water nanofluids in a car radiator. *International Journal of Thermal Sciences*, 2013, 66: 82–90.
- [10] Hussein A.M., Bakar R., Kadrigama K., Study of forced convection nanofluid heat transfer in the automotive cooling system. *Case Studies in Thermal Engineering*, 2014, 2: 50–61.
- [11] Nieh H.M., Teng T.P., Yu C.C., Enhanced heat dissipation of a radiator using oxide nano-coolant. *International Journal of Thermal Sciences*, 2014, 77: 252–261.
- [12] Teng T.P., Yu C.C., Heat dissipation performance of MWCNTs nano-coolant for vehicle. *Experimental Thermal and Fluid Science*, 2013, 49: 22–30.
- [13] Chavan D., Pise A.T., Performance investigation of an automotive car radiator operated with nanofluid as a coolant. *Journal of Thermal Science and Engineering Applications*, 2014, 6(2): 021010.
- [14] Heris S.Z., Shokrgozar M., Poorpharhang S., Shanbedi M., Noie S., Experimental study of heat transfer of a car radiator with CuO/ethylene glycol-water as a coolant. *Journal of Dispersion Science and Technology*, 2014, 35(5): 677–684.
- [15] Ebrahimi M., Farhadi M., Sedighi K., Akbarzade S., Experimental investigation of force convection heat transfer in a car radiator filled with SiO<sub>2</sub>–water nanofluid. *IJE Transactions B: Applications*, 2014, 27(2): 333–340.
- [16] Chougule S.S., Sahu S.K., Comparative study of cooling performance of automobile radiator using Al<sub>2</sub>O<sub>3</sub>-water and carbon nanotube-water nanofluid. *Journal of Nanotechnology in Engineering and Medicine*, 2014, 5(1): 010901.
- [17] Li Y., Fernández-Seara J., Du K., Pardiñas Á.Á., Latas L.L., Jiang W., Experimental investigation on heat transfer and pressure drop of ZnO/ethylene glycol-water nanofluids in transition flow. *Applied Thermal Engineering*, 2016, 93: 537–548.
- [18] Pak B.C., Cho Y.I., Hydrodynamic and heat transfer study of dispersed fluids with submicron metallic oxide particles. *Experimental Heat Transfer an International Journal*, 1998, 11(2): 151–170.
- [19] Xuan Y., Roetzel W., Conceptions for heat transfer correlation of nanofluids. *International Journal of Heat and Mass Transfer*, 2000, 43(19): 3701–3707.
- [20] Wang X.W., Xu X.F., S. Choi S.U., Thermal conductivity of nanoparticle-fluid mixture. *Journal of Thermophysics and Heat Transfer*, 1999, 13(4): 474–480.
- [21] Maxwell J.C., A treatise on electricity and magnetism, vol 1. Clarendon Press, Oxford, 1873.
- [22] Holman J.P., Gajda W.J., Experimental methods for engineers, vol 2. McGraw-Hill, New York, 2001.
- [23] Shah R.K., London A.L., Laminar flow forced convection in ducts: a source book for compact heat exchanger analytical data. *Advances in heat transfer: Supplement*. New York: Academic Press: 109. 1978.
- [24] Vajjha R.S., Das D.K., Namburu P.K., Numerical study of fluid dynamic and heat transfer performance of Al<sub>2</sub>O<sub>3</sub> and CuO nanofluids in the flat tubes of a radiator. *International Journal of Heat and Fluid Flow*, 2010, 31(4): 613–621.
- [25] Kayhani M., Soltanzadeh H., Heyhat M., Nazari M., Kowsary F., Experimental study of convective heat

- transfer and pressure drop of  $\text{TiO}_2$ /water nanofluid. *International Communications in Heat and Mass Transfer*, 2012, 39(3): 456–462.
- [26] Zeinali Heris S., Razbani M.A., Estellé P., Mahian O., Rheological behavior of zinc-oxide nanolubricants. *Journal of Dispersion Science and Technology*, 2015, 36(8): 1073–1079.
- [27] Samira P., Saeed Z.H., Motahare S., Mostafa K., Pressure drop and thermal performance of CuO/ethylene glycol (60%)-water (40%) nanofluid in car radiator. *Korean Journal of Chemical Engineering*, 2015, 32(4): 609–616.
- [28] Heris S.Z., Etemad S.G., Esfahany M.N., Experimental investigation of oxide nanofluids laminar flow convective heat transfer. *International Communications in Heat and Mass Transfer*, 2006, 33(4): 529–535.
- [29] Nassan T.H., Heris S.Z., Noie S., A comparison of experimental heat transfer characteristics for  $\text{Al}_2\text{O}_3$ /water and CuO/water nanofluids in square cross-section duct. *International Communications in Heat and Mass Transfer*, 2010, 37(7): 924–928.
- [30] Sonage B., Mohanan P., Miniaturization of automobile radiator by using zinc-water and zinc oxide-water nanofluids. *Journal of Mechanical Science and Technology*, 2015, 29(5): 2177–2185.
- [31] Mehrjou B., Heris S.Z., Mohamadifard K., Experimental study of CuO/water nanofluid turbulent convective heat transfer in square cross-section duct. *Experimental Heat Transfer*, 2015, 28(3): 282–297.
- [32] Taghizadeh-Tabari Z., Heris S.Z., Moradi M., Kahani M., The study on application of  $\text{TiO}_2$ /water nanofluid in plate heat exchanger of milk pasteurization industries. *Renewable and Sustainable Energy Reviews*, 2016, 58: 1318–1326.
- [33] Bhimani V., Rathod P., Sorathiya A., Experimental study of heat transfer enhancement using water based nanofluids as a new coolant for car radiators. *International Journal of Emerging Technology and Advanced Engineering*, 2013, 3(6): 295–302.